Proceedings of FEDSM'01
2001 ASME Fluids Engineering Division Summer Meeting
May 29- June 1, 2001-New Orleans, Louisiana

FEDSM2001-18135

STUDY OF JET IMPINGEMENT HEAT TRANSFER FOR VARYING FLUID FLOW CHARACTERICTICS

Paresh Patel and Subrata Roy
Department of Mechanical Engineering
Kettering University
Flint, Michigan 48504, USA

ABSTRACT

Certain parameters like nozzle geometry, jet impingement angle, fluid properties and nozzle-to-target plane spacing are critically important in jet impingement heat transfer process. In this paper, the fluid-thermal characteristics of an array of two rectangular jets impinging on an inclined surface are identified for varying fluid flow properties. Heat transfer modes and flow characteristics are studied for a fluid of Prandtl number 0.7 with eight Reynolds number ranging from 500 to 20000. Nusselt number, turbulent intensity and wall y^+ distributions are compared with closed and open boundary conditions on three specified lines located on the inclined surface. Velocity components are also compared on a horizontal line passing through the center of the inlet nozzle.

INTRODUCTION

Jet impingement heat transfer has been employed in many practical applications for cooling and drying because of its easy implementation and high heat transfer rate. Examples include turbine blade film cooling, bearing cooling, electronics cooling, vehicle windshield deicing/defogging, drying of paper, and glass tempering. In many of these applications, the Nusselt number (Nu) distribution resulting from the jet attachment to the target plate, the trajectory and physical properties of the jet are critical design parameters. The specific application of interest is air issuing from the nozzles consisting of two rectangular jets and impinging upon an inclined plate.

Impingement of single and multiple jets on surface has been extensively investigated in the literature. Impingement of single circular jet on perpendicular and inclined plate in Lamont and Hunt (1979) showed surface pressure distribution on entire impingement region for varying plate angles ranging from 30 to 90 and pressure ratios. Bernard et al., (1999) studied several (fifteen) jets impinging on a plane wall to describe the flow near the impinged plate using various experimental techniques. Polat et al. (1989) presented a relatively recent review of numerical studies related to axisymmetric impinging jets. More reviews were also documented by Martin (1977a), and Downs and James (1987). Lee et al. (1994) showed local heat transfer from an elliptical jet impingement on a flat plate. An array of elliptical jets (Arjocu and Liburdy, 2000) has been studied extensively to understand the dominant modes associated with the local heat transfer coefficient distribution for low Reynolds number (Re) such as 300 and 1500, while Martin (1977b) has identified optimum impingement and separation distances for heat transfer for larger Reynolds number ($2500 \leq Re \leq 4{,}000{,}000$).

Pan and Webb (1994) studied local heat transfer details of the circular jet array impingement. Metzger et al. (1974) has investigated the effect of Prandtl number (Pr) on jet impingement heat transfer characteristics while Rahman et al. (1998) has identified conjugate heat transfer during free jet impingement of a high Pr fluid. Leland and Pais (1999) obtained heat transfer coefficients for high Pr fluid ranging from 48 to 445 and jet Re of 109 to 8592. Morris et al. (1996) has studied local heat transfer coefficient distribution on the plate due to a normally impinging jet of Reynolds Number ranges from 8500 to 13,000. Roy et al. (2001) has compared numerical and experimental results for temperature and local heat transfer coefficient distribution on the surface impinging upon an array of two rectangular jets. In this paper, authors study the jet impingement flow characteristics and investigate the effect of Reynolds number on local and average Nusselt number, turbulence intensity (TI) and wall y^+. Authors also discuss the effect of the Reynolds Number on the velocity component u, v and w on a line d passing through the control volume as shown in figure 1.

Figure 1 describes schematic of the jet, the inclined surface and its association with the control volume bounded by sidewalls, roof wall, bottom wall and back wall. All necessary dimensions are given in the figure. The jet is issued at temperature T_j, normal to the nozzle exit plane, through two rectangular openings (hxw) impinging upon the target plane of thickness t. The target plane is inclined at an angle of α so that

the jet impingement angle is (90-α). The mean velocity of the jet *V* depends on the jet Reynolds number and the hydraulic diameter of the inlet nozzle.

Heat transfer process in computational domain is investigated by using a finite volume based commercial code FLUENT©. The three-dimensional computational model is analyzed with renormalized group (RNG) k-ε turbulence closure model to get Nu distribution on the inside of the inclined surface. Comparison between the local and average Nu distribution on the surface for closed and open boundary conditions are also reported. In this work, Nu distribution over the inclined surface is compared for eight jet Reynolds numbers (Re=500, 1500, 5000, 7500, 10000, 12500, 15000 and 20000) for a fluid of Prandtl number 0.7 (e.g. air).

NOMENCLATURE

k Turbulent kinetic energy
p Pressure
t Time
x_i partial derivative in space
u_i Cartesian velocity component
u_j Cartesian velocity component
y Distance between the wall and nearest node
C_i Coefficients
y^+ Inner variable
H Enthalpy
u_τ Wall shear velocity
S_{ij} mean strain tensor
Pr Prandtl Number

Greek
ε Dissipation rate of turbulent kinetic energy
μ_t Eddy viscosity
μ Viscosity
ρ Density
τ_{ij} Stress tensor
δ_{ij} Kronecker delta

Subscripts
eff effective
avg Average
k Mean velocity
i,j Direction of special derivatives
τ Shear stress based variable
w Wall

THEORITICAL FORMULATION

Governing Equations

For solving the standard variables u, v, w, k, ε and T, three-dimensional Navier-Stokes equations for steady, turbulent and incompressible flow can be written as in Roy (2000),

Mass (Continuity) Equation:

$$\frac{\partial r}{\partial t}+\frac{\partial}{\partial x_i}(ru_i)=0 \quad \text{.....(1)}$$

Momentum Equation:

$$\frac{\partial}{\partial t}(ru_i)+\frac{\partial}{\partial x_j}(ru_iu_j)+\frac{\partial p}{\partial x_i}-\frac{\partial t_{ij}}{\partial x_j}=0 \quad \text{.....(2)}$$

Energy Equation:

$$\frac{\partial}{\partial t}(rH)+\frac{\partial}{\partial x_j}(ru_iH-u_it_{ij})=0 \quad \text{.....(3)}$$

Where the stress tensor τ_{ij},

$$t_{ij}=\left[m\left(\frac{\partial u_i}{\partial x_j}+\frac{\partial u_j}{\partial x_i}\right)\right]-\frac{2}{3}m\frac{\partial u_i}{\partial x_i}d_{ij}$$

Turbulence Modeling:

Renormalization group (RNG) based standard k-ε turbulence model (Yakhot and Orszag, 1986) contains two equations one for turbulence kinetic energy and the other for its dissipation rate obtained from the following equations respectively,

$$r\frac{\partial k}{\partial t}=\frac{\partial}{\partial x_i}\left[\left(m+\frac{m_t}{\mathrm{Pr}_k}\right)\frac{\partial k}{\partial x_i}\right]+\left(2m_tS_{ij}-\frac{2}{3}rkd_{ij}\right)\frac{\partial u_j}{\partial x_i}-re \quad \text{....(4)}$$

and

$$r\frac{\partial e}{\partial t}=\frac{\partial}{\partial x_i}\left[\left(m+\frac{m_t}{\mathrm{Pr}_k}\right)\frac{\partial e}{\partial x_i}\right]+C_{1e}\frac{e}{k}\left(2m_tS_{ij}-\frac{2}{3}rkd_{ij}\right)\frac{\partial u_j}{\partial x_i}-C_{2e}r\frac{e^2}{k} \quad \text{.....(5)}$$

In the above equation three terms on the right hand side shows the diffusion, generation and dissipation rates of ε and Turbulent viscosity derived is,

$$m_t=C_m r\frac{k^2}{e}$$

where C_μ=0.0845 (Lam,1992).

Accurate computation of the turbulent flow strongly depends on the local grid generation especially in the near wall region where the shear layer forms. In this region, the mesh measure can be computed as,

$$y^+=\frac{ru_ty}{m} \quad \text{.....(6)}$$

where $u_t=\sqrt{t_w/r}$ and y is the normal distance from the wall.

Boundary Conditions

Two different boundary conditions (BCs) are applied to analyze the fluid thermal systems. In one BC, the side walls,

roof wall, bottom wall and back wall of the control volume are considered as typical wall boundary conditions. Here onwards, this will be called 'closed BC'. In the other, all boundaries except for the inclined plane and inlet jets are pressure outlet i.e. atmospheric pressure boundary condition. Here onwards, we call this 'open BC'. The inclined plane is always considered as no-slip wall where a convective boundary condition with constant temperature of 273 K and a heat transfer coefficient of 35 W/m^2 K is applied. Jet at 293 K is issued from the nozzle exit plane with a plug flow velocity V that was imposed by 500 ≤Re≤ 20000.

RESULTS AND DISCUSSION

Figure 1 shows schematic of the computational domain which has been discretized in 181,000 tetrahedral finite volumes using commercial modeling code Hypermesh® 3.1. The three dimensional Navier-Stokes equations (1)-(5) are then solved using Fluent© 5.2 for flow, energy and turbulence closure. For understanding heat transfer process and flow characteristics, three lines a, b and c with constant z-coordinate 0.3733m, 0.5233m and 0.7233m, respectively, are selected along the height H of the inclined plane. These lines coincide with the plane between the jet and sidewall, axis of the jet, and between the jets. The Nusselt number, turbulence intensity and wall y^+ distribution on these three lines are investigated in this section. Line d with constant y-coordinate 0.082m, starts from the point where jet axis impinges on the surface and ends on a point of back wall as shown in figure 1. Velocity components u, v and w are studied on this line d to investigate flow characteristics.

Figure 2 shows the trend of average Nusselt number (Nu_{avg}) on the surface for different Re with open and closed boundary conditions. In general, Nu_{avg} increases as the Re increases. It is also higher for closed BC than for open BC. The jet-vortex interaction appears to have a significant effect on heat transfer. For closed BC, the trendline shows $Nu = 1.74\ Pr^{1/3}\ Re^{0.5962}$, while for open BC, the relationship is $Nu = 0.024\ Pr^{1/3}\ Re^{0.9888}$. Figure 3 shows particle track from inlet colored by velocity magnitude in the computational domain for closed boundary condition. It shows formation of small bound vortices in between two rectangular inlet openings because of large velocity magnitude, while after impingement of the jet with solid surface it creates a smaller wake upstream and a larger wake in the downstream region. Figure 4 shows the same for open boundary conditions and does not show any flow recirculation except for small bound vortices formation.

Turbulence intensity (TI) plays a critical role in identifying the level of turbulence kinetic energy in the solution domain. Figure 5 shows TI distribution on lines a, b and c to understand the fluid flow nature. It is highest at stagnation point showing mean velocity gradient is the highest at the stagnation point and sharply decreasing in the nearby region where the shear layer forms. Contrary to Nu_{avg}, TI is generally higher for open BC than for close BC. Figure 6 shows comparison of Nu distribution on the lines a, b and c for 500≤Re≤20000 with close (adiabatic wall) and open (pressure outlet) boundary conditions for roof, bottom, back and side walls of the control volume. Nusselt number is a function of local heat transfer coefficient as the reference length and thermal conductivity remains constant for a particular fluid. Thus its distribution gives better idea of jet impingement heat transfer modes through the surface. The highest value of Nu

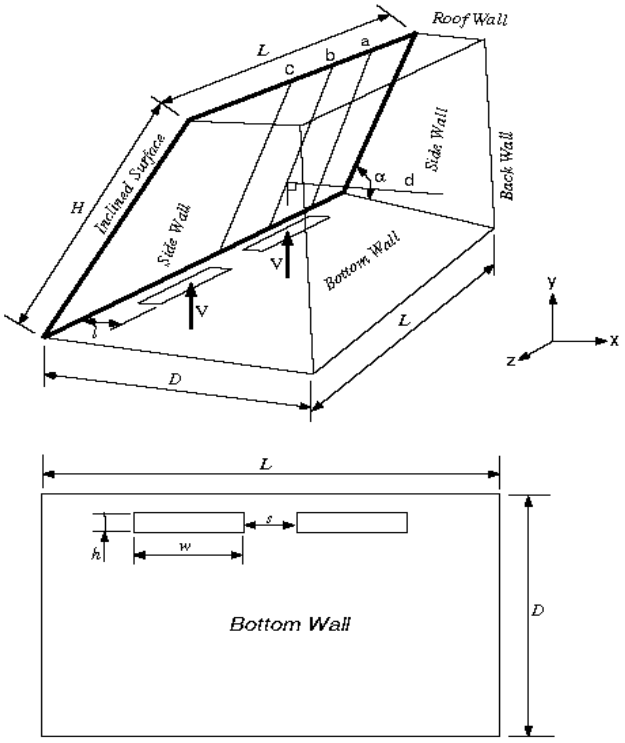

Name	Dimensions (m)
Length of inclined surface, L	1.447
Width of inclined surface, H	0.719
Surface inclination angle, α	30°
Surface thickness, t	0.006
Length of nozzle exit plane, h	0.019
Width of nozzle exit plane, w	0.241
Distance between nozzle exit planes, s	0.127

Figure 1. Schematic of the computational domain.

occurs at the stagnation point (intersection of the jet axis and the inclined surface) and decreasing in its nearby region where shear layer forms.

At the stagnation point the diffusive heat transfer is dominant and in its nearby region the convective heat transfer is dominant because of higher velocity gradient. For all Re, the peak Nusselt number in closed BC is always higher than that

for open BC. This is primarily due to the fact that more energy is lost in open BC than in closed adiabatic BC. Also peak Nu increases as Re increases.

Wall Y-plus is a function of wall shear stress in the, if we consider the distance between the wall and nearest node constant. Figure 7 shows the distribution of Wall Y-plus on the lines a, b and c to demonstrate wall shear stress distribution. Wall Y-plus is fluctuating but its peak is at stagnation point and decreases slowly in its nearby region means maximum wall shear stress is producing at stagnation point and its decreases slowly in the nearby region. Moreover, it is higher for open BC than close BC means higher wall shear stress is producing for open BC than close BC for the same Reynolds Number.

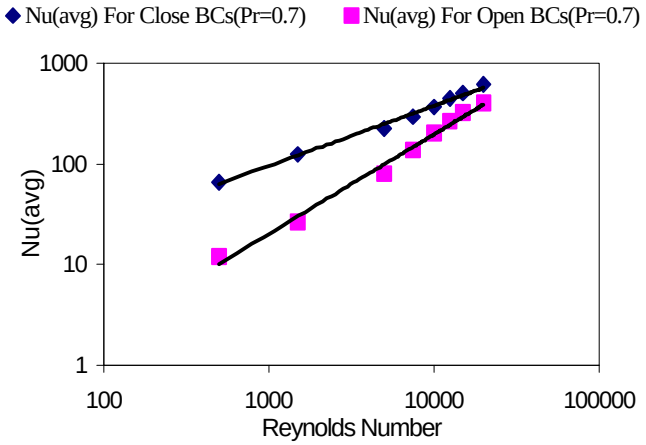

Figure 2. Comparison of average Nu vs Re.

Figure 8 documents the comparison of velocity components for closed BC with open BC on line d parallel to the x-axis (see figure 1) for Re=5000. The flow component w shows maximum noticeable difference as the closed BC shifts between –0.02 to 0.11m/s while the open BC fluctuates in the negative (-0.05, 0. m/s) region. Figure 9 plots similar result for Re=20000. As the Reynolds number increases, the u and v components intensify; however, the w for open BC becomes positive downstream of the inlet.

CONCLUSIONS

Jet impingement heat transfer and flow characteristics for two rectangular jets impinging upon an inclined surface have been studied with the following conclusions.

- Heat transfer is maximum through the shear layer formed near the jet attachment stagnation region.
- For all Re, the peak Nusselt number in closed BC is higher than open BC. This is primarily due to the fact that more energy is lost in open BC than in closed adiabatic BC.
- Turbulence (velocity gradient) and wall shear force is higher in the shear layer region and highest at stagnation point.
- Average Nu increases as Re increases.

ACKNOWLEDGMENTS

First author of this paper thankfully acknowledges Kettering University for giving an opportunity to work as a Graduate Research Assistant.

REFERENCES

Arjocu, S.C. and Liburdy, J.A., 2000, "Identification of Dominant Heat Transfer Modes Associated With the Impingement of an Elliptical Jet Array." *Journal of Heat Transfer, vol.122, pp 240-247.*

Morris, G.K., Garimella, S.V. and Amano, R.S., 1996, "Prediction of Jet Impingement Heat Transfer Using a Hybrid Wall Treatment With Different Turbulent Prandtl Number Functions," *Journal of Heat Transfer, vol.118, pp 562-568.*

Leland, J.E. and Pais, M.R., 1999, "Free Jet Impingement Heat Transfer of a High Prandtl Number Fluid Under Conditions of Highly Varying Properties." *Journal of Heat Transfer, vol.121, pp 592-597.*

Roy, S., Nasr, K., Patel, P. and Bashar, A., 2001, "Heat Transfer on a Vehicle Windshield: An Experimental and Numerical study." *Proceedings of National Heat Transfer Conference, Paper no. NHTC01-1113.*

Lee, S.J., Lee, J.H. and Lee, D.H., 1994, "Local Heat Transfer Measurements from an Elliptical Jet Impinging on a Flat Plate using liquid Crystal." *International Journal of Heat and Mass Transfer, 37, No.6, pp.967-976.*

Martin, H., 1977a, "Heat and Mass Transfer Between Impinging Jets and Solid Surfaces." *Adv. Turbulence, vol.2 pp.37-44.*

Pan, Y. and Webb, B.W., 1994, "Visualization of Local Heat Transfer Under Arrays of Free-Surface Liquid Jets. "*Proc. of the 10th International Heat Transfer Conference, vol.4, pp. 77-82.*

Metzger, D.E., Cummings, K.N. and Ruby, W.A., 1974, "Effects of Prandtl Number on Heat Transfer characteristics of Impinging Liquid Jets." *Proceeding of the 5th International Heat Transfer Conference, vol.2, pp.20-24.*

Rahman, M.M., Bulla A.J. and Leland J.E., 1998, " Numerical model of Conjugate Heat Transfer during Free Liquid Jet Impingement." *Proc. of the ASME, AES-vol.38, pp.475-486.*

Lamont P.J. and Hunt B.L., "The impingement of under expanded, axisymmetric jets on perpendicular and inclined plates." *Journal of Fluid Mechanics 1980, vol. 100, part 3, pp. 471-511.*

Benard A., Brizzi L.E. and Bousgarbies J.L., 1999, "Study of Several Jets Impinging on a Plane Wall: Visualizations and Laser Velocimetry Investigations." *Journal of Fluid Engineering, vol.121, pp.808-812.*

Downs, S. J. and James, E. H., 1987, "Jet impingement Heat Transfer—a Literature Survey", *ASME Paper No. 87-HT-35.*

FLUENT© 5 User's Guide, Fluent Inc., 1998, Volume 1-4, Lebanon, NH.

Hyperworks© 4.0 Online Users Manual, 2000, Altair Engineering, Troy, MI.

Lam, S. H., 1992, "On the RNG Theory of Turbulence," *Physics of Fluids A, Vol. 4, pp. 1007-1017.*

Martin, H., 1977b, "Heat And Mass Transfer Between Impinging Gas Jets And Solid Surfaces". *In Advances in Heat Transfer, Academic Press, New York, Vol. 13. pp. 1-60.*

Polat, S., Huang, B., Mujumdar, A.S., and Douglas, W.J.M., 1989, "Numerical Flow and Heat Transfer Under Impinging Jets: A Review," *Annual Review of Numerical Fluid Mechanics and Heat Transfer, Vol.2 pp.157-197.*

Roy, S., 2000, "Numerical Investigation Of The Blade Cooling Effect Generated By Multiple Jets Issuing At An Angle Into An Incompressible Horizontal Cross Flow," *Numerical Heat Transfer – Part A, Vol. 38, no. 7, pp. 701-718.*

Yakhot, V. and Orszag, S.A., 1986, "Renormalization Group Analysis Of Turbulence. I. Basic Theory," *Journal of Scientific Computing, Vol. 1, pp. 3-51.*

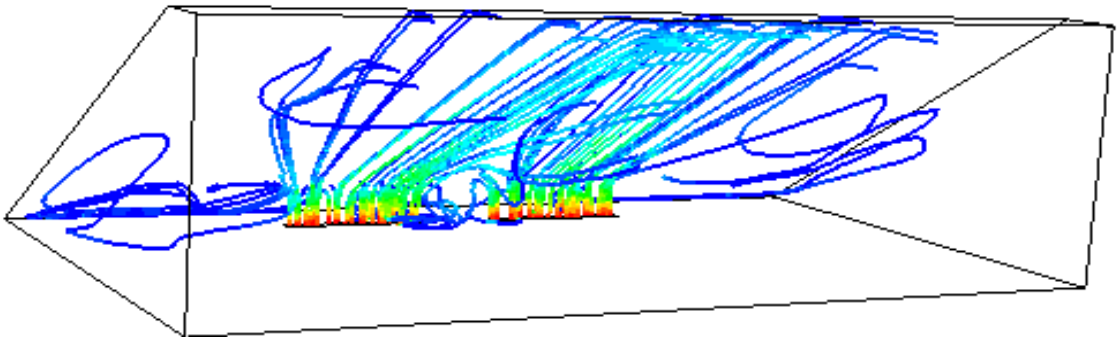

Figure 3. Path lines showing the particle track in the computational domain for close boundaries, for Re=12500.

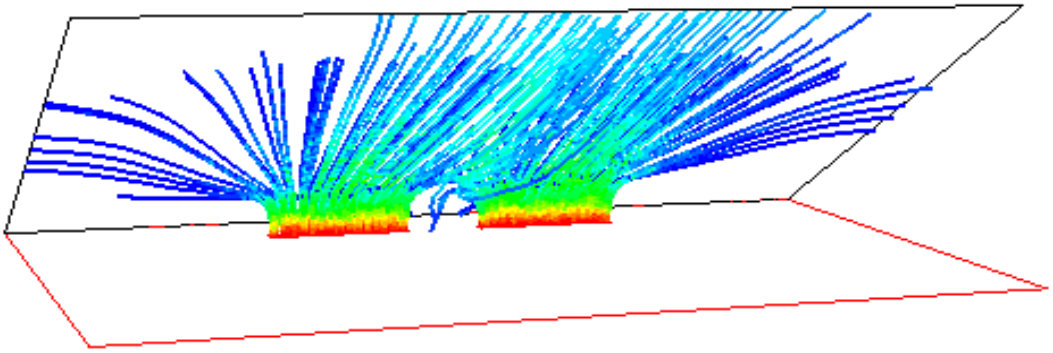

Figure 4. Path lines showing the particle track in the computational domain for open boundaries, for Re=12500.

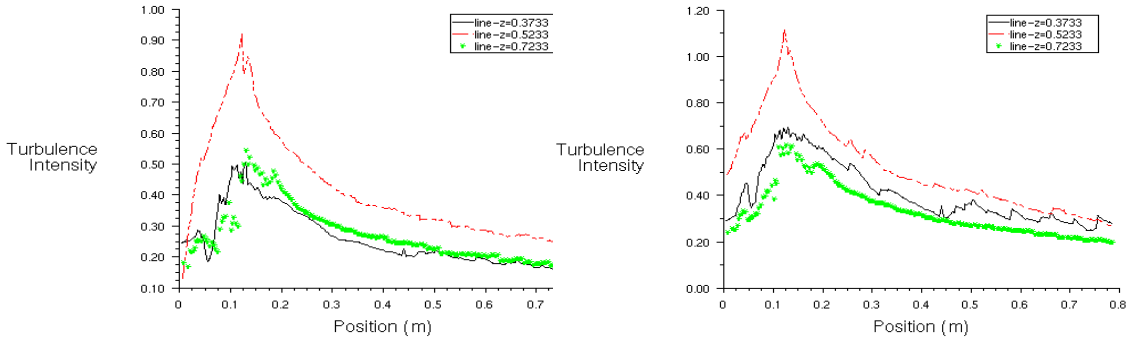

Figure 5. Comparison of Turbulence Intensity distribution over the surface for open and close boundary conditions, Re=20000, Pr=0.7.

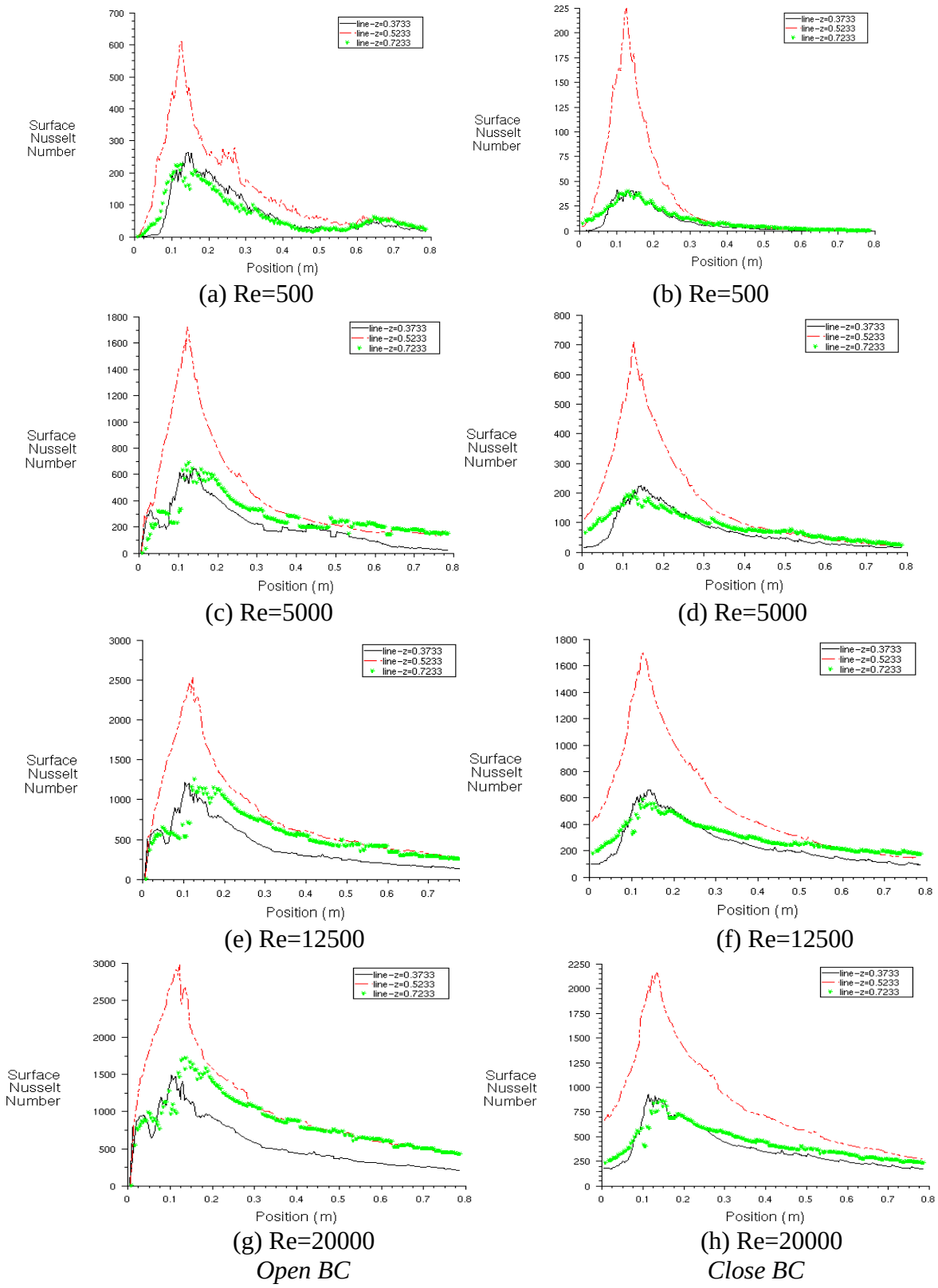

(a) Re=500 (b) Re=500

(c) Re=5000 (d) Re=5000

(e) Re=12500 (f) Re=12500

(g) Re=20000 *Open BC* (h) Re=20000 *Close BC*

Figure 6.Comparision of Nusselt Number distribution over the surface for open and close boundary conditions, Pr=0.7.

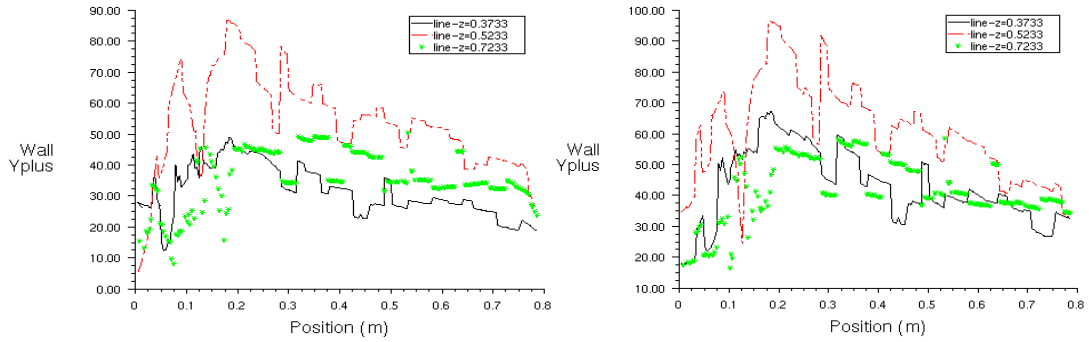

(a) Re=20000 *Open BC*

(b) Re=20000 *Close BC*

Figure 7.Comparison of Yplus (y^+) distribution over the surface for open and close boundary conditions, For Pr=0.7.

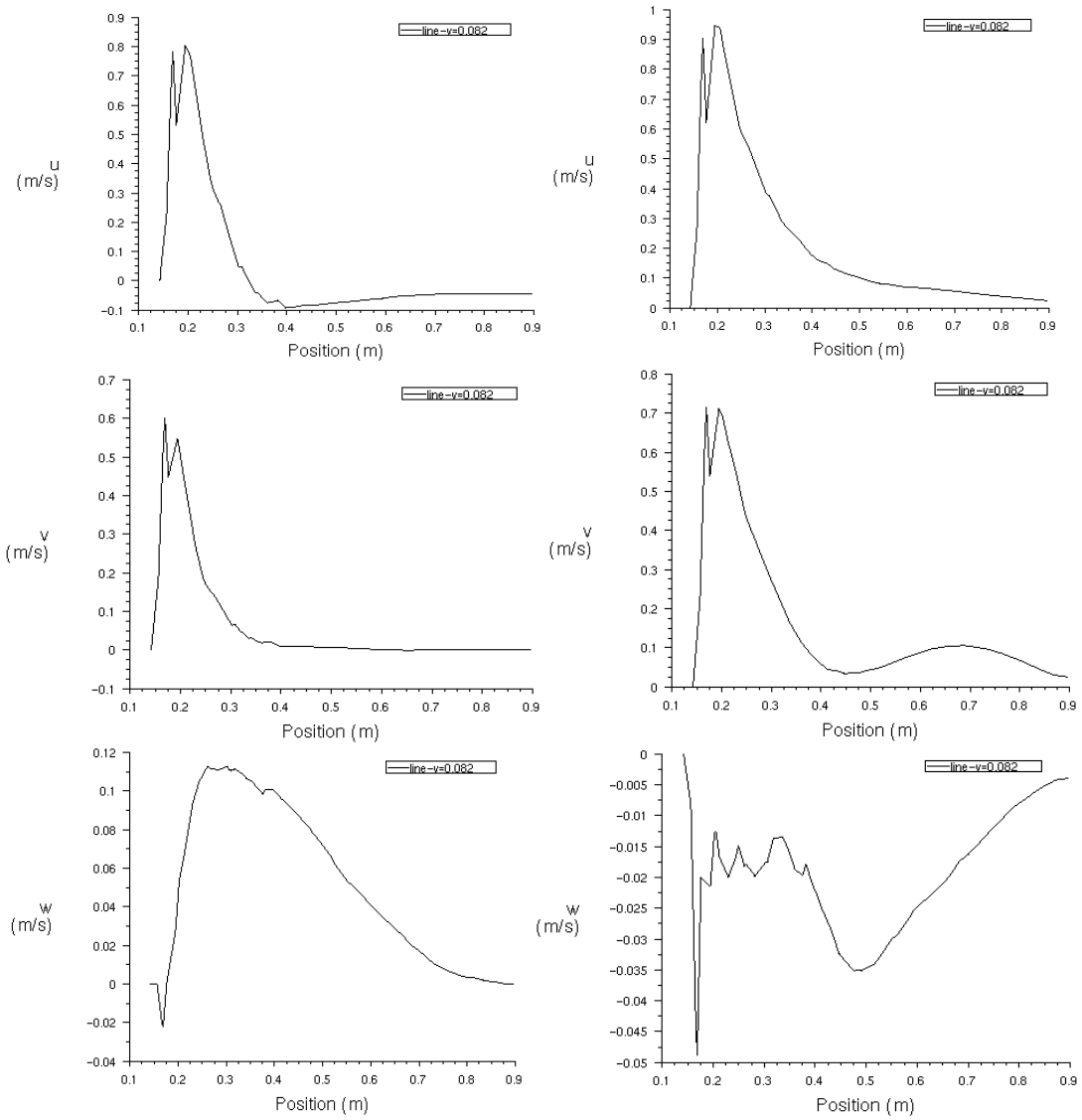

Close BC *Open BC*

Figure 8. Comparison of u, v and w velocity components along the line d for Re=5000.

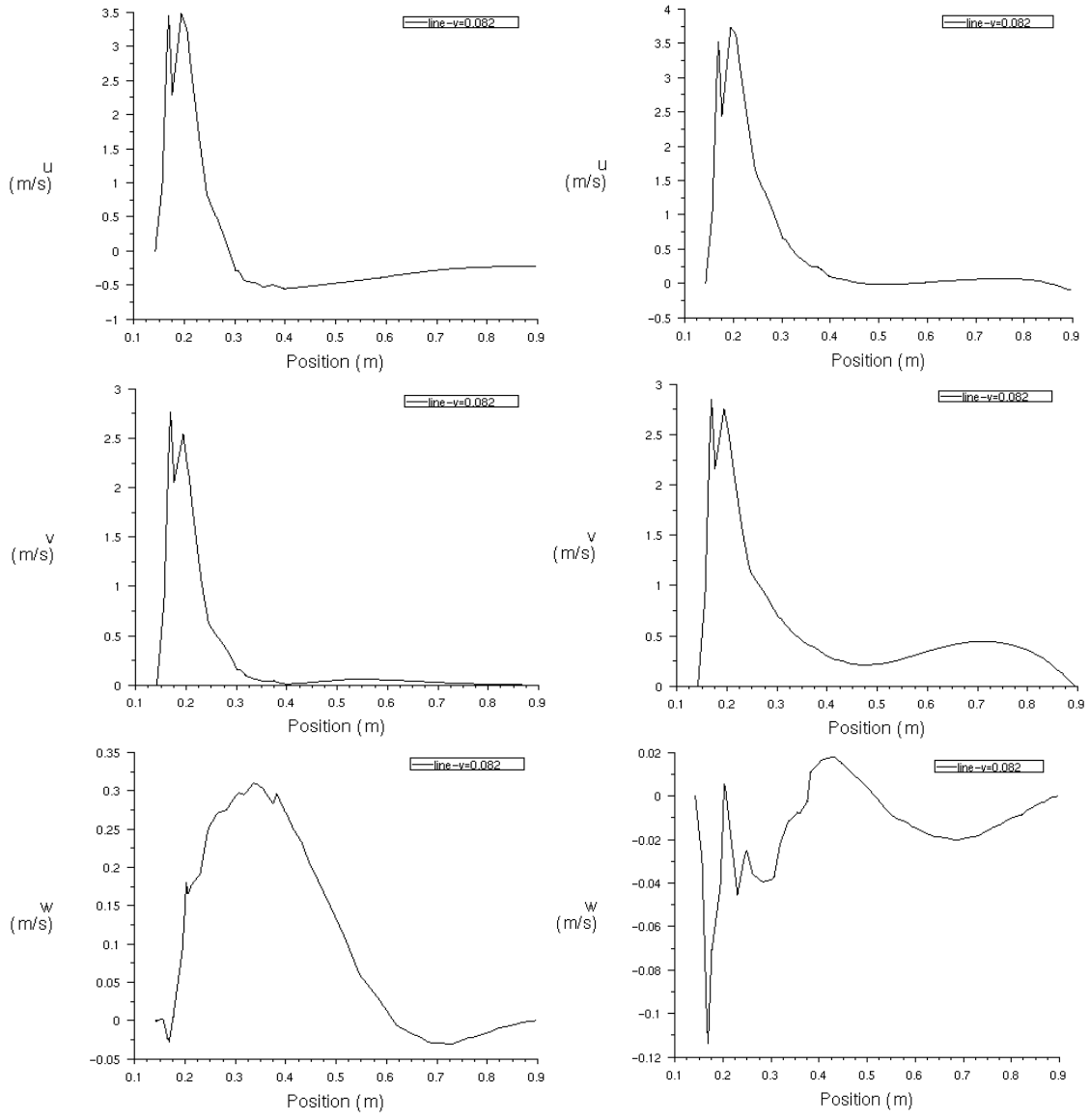

Close BC Open BC

Figure 9. Comparison of u, v and w velocity components along the line d for Re=20000.